

# Exact moments for a run and tumble particle in a harmonic trap with a finite tumble time

Aoran Sun,<sup>1,2</sup> Fangfu Ye,<sup>1,2,3</sup> and Rudolf Podgornik<sup>2,1,3,4,\*</sup>

<sup>1</sup>Beijing National Laboratory for Condensed Matter Physics,  
Institute of Physics, Chinese Academy of Sciences, Beijing 100190, China

<sup>2</sup>School of Physical Sciences, University of Chinese Academy of Sciences, Beijing 100049, China

<sup>3</sup>Wenzhou Institute, University of Chinese Academy of Sciences, Wenzhou, Zhejiang 325001, China

<sup>4</sup>Kavli Institute for Theoretical Sciences, University of Chinese Academy of Sciences, Beijing 100049, China

We study the problem of a run and tumble particle in a harmonic trap, with a finite run and tumble time, by a direct integration of the equation of motion. An exact 1D steady state distribution, diagram laws and a programmable Volterra difference equation are derived to calculate any order of moments in any other dimension, both for steady state as well as the Laplace transform in time for the intermediate states. We also use the moments to infer the distribution by considering a Gaussian quadrature for the corresponding measure, and from the scaling law of high order moments.

## I. INTRODUCTION

Unlike Brownian particles that only move when passively driven by an external force, active particles can be driven by energy provided by the environment, fueling their motion [1–3]. Many vivid examples of active particles can be found either in nature, such as molecular motors [4, 5], cells [6, 7], granular materials [8], active gels [9, 10], large (compared with cells) animals [11–14], etc., or fabricated with robot-like qualities [2, 15, 16].

Active particles have attracted substantial interest also theoretically, due to nonequilibrium, non-Boltzmann statistics [15–17], even in the case of a single particle in free space. Run and tumble particle (RTP) is one such simple model that mimics the actual motion of a certain type of active particles like bacteria, *e.g.*, *Escherichia coli* [6, 18, 19]. In this model, the active particle moves with constant velocity for an exponentially distributed time (*the run state*), and then randomly changes its velocity (*the tumble state*) to another, randomly chosen velocity of the same magnitude (another run state). Despite the apparent simplicity, such model already contains rich features and can be non-trivial to analyze [17, 20, 21]. At a single particle level, time dependent distribution has been found for the general case (in terms of its Fourier-Laplace transform) [22], while for many interacting particles, interesting features including boundary clustering [2], phase separation [23], and jamming [24], have been observed. Other interesting quantities, such as first passage time [21, 25], survival probability [21], distribution of the time of maximum [26], have also been calculated.

An active particle, and more specifically, an RTP in an external potential is a natural and interesting generalization of this problem [27–29]. It may eventually reach a non-Boltzmann, nonequilibrium steady state [30–33]. For the special case of a harmonic potential, the exact steady state distribution for RTP in 1D [34, 35] and 2D [31–33] have been found, as well as the moments of the steady state distribution in the 3D case [31–33].

This model has been further generalized by including

a random velocity for run states [36], a space-depending run rate [28, 37], a non-exponential time between tumbles [29], as well as stochastic resetting to a starting point [38, 39].

In general, the theoretical analysis of the RTP model, especially in the presence of an external field, can be very challenging. Except for the case when an exact solution is available, or a perturbation analysis is applicable [40–42], many problems still seem to be beyond what is currently feasible.

Most of the recent theoretical approaches assume that the tumble time is zero, *i.e.*, the particle starts another run immediately after one run, and thus always exhibits a non-zero active velocity. In contrast, *Escherichia coli* is observed to have a tumble state with small but finite time between active runs, during which the cell mainly rotates and has nearly zero net motion [6]. In free space, such a state is relatively easy to take into account and time depending distribution has been found in general (in terms of its Fourier-Laplace transform) [22]. In the presence of an external potential, however, the only theoretical result seems to be a 1D case with a harmonic potential, where average time in run and tumble states are equal [43]. This special case is essentially a direct product of two 1D RTP projected back to 1D [30].

It has been found recently [31–33] that, although the steady state distribution for 2D and 3D RTP in a harmonic trap is difficult to derive, one can obtain an exact recursive relation for the moments of such a distribution by partially integrating the Fokker-Planck equation. Furthermore, in 2D, one can easily infer the moments, and even obtain the exact steady state distribution from the moments. Guided by the seminal work of Mark Kac [44], we integrated the equation of motion directly in order to obtain the moments of the steady state distribution function of an RTP in a harmonic trap with finite exponentially distributed tumble time. We derive the diagram laws to directly calculate the moments for steady state, or the Laplace transform in time for moments at any time, with arbitrary run time as well as tumble time, in any dimension. From the diagram laws we can find

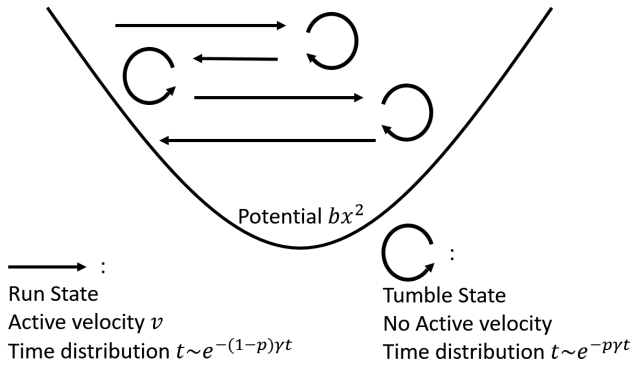


Figure 1. Schematic drawing of the 1D case of the problem considered in this work. While the drawing represents 1D for clarity, the method here works for 2D and 3D as well. The velocity of the particle has two components, the pull  $-bx$  of harmonic potential  $bx^2$ , depending only on the position, and active velocity, which switches randomly between zero (*the tumble state*), and a vector of magnitude  $v$  along a randomly chosen direction (*the run state*). The time between switches is exponentially distributed, with rate  $(1-p)\gamma$  and  $p\gamma$ , respectively for run and tumble state, and each choice of the active velocity at the beginning of each run state is independent from space, time, or previous choices.

a Volterra difference equation [45] which can be programmed to recursively calculate the moments.

Furthermore, in 1D we can obtain an exact steady state distribution, and are thus able to extend the result from [43] to the case when run time and tumble time are different.

The rest of the paper is organized as follows. In Section II, we define our model and describe our method. In Subsection IIA we obtain one set of equations of motion for our model. We then briefly describe the method to calculate the moments in Subsection IIB. The programmable Volterra difference equation is given in Subsection IIC, and in Subsection IID we consider some general results, such as the zero potential limit, properties of the density at the boundary. We also briefly mention how the method can be adapted to Active Brownian particles in Subsection IIE. In Section III, we consider the special case of 1D, and present an exact steady state distribution for arbitrary run time and tumble time. In Section IV we deduce the distribution from its moments. Finally, in Section V we list the conclusions, where we summarize the results with a discussion of the possible extensions based on the general methodology described in the previous sections.

$R(m)$	$R(m-1) = 0$	$R(m-1) \neq 0$
$p$	random points	$R(m-1)$
$1-p$	0	0

Table I. Definition of  $R(m)$ . With the value of  $R(m-1)$  given in the first row,  $R(m)$  may take a value from the corresponding column, with probability given by the first column. So the table reads,  $\mathbb{P}(R(m) = R(m-1) | R(m-1) \neq 0) = p$ ,  $\mathbb{P}(R(m) = 0 | R(m-1) \neq 0) = 1-p$ ,  $\mathbb{P}(R(m) = 0 | R(m-1) = 0) = 1-p$ , and if  $R(m-1) = 0$  there is probability  $p$  that  $R(m)$  takes a new random value according to our model.

## II. METHOD OUTLINE

### A. Equation of motion

We consider a general motion in  $d$  dimensional space, by looking at a single coordinate component, which contains the most vital information in the spherical symmetry. We model the RTP with finite tumble time, during which the velocity of the particle has no active component, but only the passive component from the external potential) with the following equation:

$$\dot{x}(t) = -bx(t) + vR(N(t)) \quad (1)$$

where  $R(N(t))$  stands for (the projection onto one coordinate axis of) the dimensionless active velocity process,  $x$  is the same coordinate component of the position, while  $b$  is the strength of the harmonic trap and  $v$  is the magnitude of the active velocity, both considered as constants.  $N(t)$  is a Poisson process with a constant rate  $\gamma$ :

$$P(N(t) = n) = \frac{(\gamma t)^n e^{-\gamma t}}{n!} \quad (2)$$

$R$  is a Markov chain of an integer variable, defined in the following way: the value of  $R(m)$  is randomly chosen according to the previous value  $R(m-1)$ . If  $R(m-1) \neq 0$ , then there is probability  $p$  that  $R(m) = R(m-1)$  and thus the particle retains the same active velocity, and probability  $1-p$  that  $R(m) = 0$  and the particle enters the tumble state; otherwise, if  $R(m-1) = 0$ , there is probability  $p$  that  $R(m)$  takes a new random value according to our model, independent from previous values of  $R$ , and there is probability  $1-p$  that  $R(m) = 0$  and the particle remains in the tumble state. The definition is summarized in Table I.

In this way, both run and tumble have exponentially distributed time with rate  $\gamma_R = (1-p)\gamma$  and  $\gamma_T = p\gamma$  respectively. This can be shown with brutal force calculation, e.g., the time in one run state  $\tau$  satisfies:

$$\mathbb{P}(\tau > t) = \sum_{n=0}^{\infty} P(N(t) = n) n^p = e^{-(1-p)\gamma t} \quad (3)$$

and the distribution density can be obtained by taking the derivative w.r.t  $t$ . Note that  $\mathbb{P}(R(m) = 0) = 1 - p$  for all  $m > 0$ . We require that the initial condition should also be  $\mathbb{P}(R(0) = 0) = 1 - p$ .

The random points are model dependent. In general they could be taken from any distributions, but in this work we focus on the RTP, where the (dimensionless) active velocity is randomly and uniformly chosen from a unit sphere in  $d$  dimension  $S^{d-1}$ . Since we are working with only the  $x$  coordinate component, we project the active velocity onto the  $x$  coordinate axis. The distribution for the square of the projected active velocity (conditioned on when it is non-zero)  $y = (R(m))^2$  is:

$$p(y) = \frac{\Gamma\left(\frac{d}{2}\right) (1-y)^{\frac{d-3}{2}}}{\sqrt{\pi y} \Gamma\left(\frac{d-1}{2}\right)} \quad (4)$$

Since  $R(N(t))$  is a simple function, we may solve Eq. 1 as an ODE:

$$x(t) = x(0) e^{-bt} + v \int_0^t R(N(s)) e^{-b(t-s)} ds \quad (5)$$

A first observation from the solution Eq. 5 is that, since  $R(N(s)) \leq 1$ ,  $|x(t)| < v/b$  unless  $|x(0)| > v/b$  and  $t$  is

small. Indeed, this can be proved by taking the absolute value of Eq. 5:

$$\begin{aligned} |x(t)| &\leq |x(0)| e^{-bt} + v \int_0^t e^{-b(t-s)} ds \\ &< |x(0)| e^{-bt} + \frac{v}{b} \end{aligned} \quad (6)$$

Intuitively, this can also be expected from the equation of motion Eq. 1. Suppose  $x > v/b$  at some moment, then Eq. 1 tells us  $\dot{x} < 0$ , and thus the particle will be pulled back towards the region  $|x| < v/b$  whatever active velocity the particle has. If  $x = v/b$  then  $\dot{x} \leq 0$ , the particle can stay at the boundary but cannot move out. Furthermore, if  $0 < x < v/b$ , then the particle might move outward, but the closer to the boundary, the slower its maximum possible velocity. So it is to be expected that the particle might not have enough active velocity to leave the region  $|x| < v/b$ .

With the solution Eq. 5, by interchanging the order of the averaging and the integration, it is possible to calculate the moments. As we are mostly interested in the long time behavior, we therefore simplify the problem by assuming  $x(0) = 0$ . The moments of the probability distribution at time  $t$  can then be written generally as:

$$\langle x(t)^{2l} \rangle = v^{2l} (2l)! \int_{0 \leq s_1 \leq t_1 \leq \dots \leq t_l \leq t} dt_i ds_i e^{-b(2lt - \sum_k (t_k + s_k))} \left\langle \prod_{k=1}^l R(N(t_k)) R(N(s_k)) \right\rangle \quad (7)$$

where we have used the symmetry to re-order the terms according to their time.

## B. Diagram laws

To evaluate these moments, we need to know the correlation function of the active velocities  $\left\langle \prod_{k=1}^l R(N(t_k)) R(N(s_k)) \right\rangle$ . A detailed derivation can be found in SI. Here it is sufficient to know that the correlation function of order  $2l$  can be calculated by summing over the conditional expectations of  $2^{l-1}$  individual cases, each one represented by a diagram of  $2l$  vertices on a line. Each vertex on a line represents a time,  $t_i$  or  $s_i$ , in the correlation function expression, and  $R$  remains the same between the times represented by the connected vertices. Furthermore the contributions of all the cases to the correlation function can be systematically calculated.

We relegated the details to the SI and only offer an example here. The correlation function of order eight contains the following diagram:

$$\bullet_{t_4} - \bullet_{s_4} - \bullet_{t_3} - \bullet_{s_3} \quad \bullet_{t_2} - \bullet_{s_2} \quad \bullet_{t_1} - \bullet_{s_1} \quad (8)$$

which represents the case that  $R$  remains the same from

$s_3$  to  $t_4$ , from  $s_2$  to  $t_2$ , and from  $s_1$  to  $t_1$ , but changes its value at least twice, first at some time between  $s_2$  and  $t_1$ , and again between  $s_3$  and  $t_2$ . The contribution from this diagram Eq. 8 to the correlation function of order eight amounts to:

$$p e^{-\gamma_R \sum_k (t_k - s_k)} P(s_3, t_2) P(s_2, t_1) e^{-\gamma_R (s_4 - t_3)} M_d^2 (M_d^1)^2 \quad (9)$$

with

$$P(s_k, t_{k-1}) = p + (1-p) e^{-\gamma(s_k - t_{k-1})} - e^{-(1-p)\gamma(s_k - t_{k-1})} \quad (10)$$

$$M_d^k = \left\langle R(N(t))^{2k} | R(N(t)) \neq 0 \right\rangle = \frac{\Gamma(1/2 + k) \Gamma(d/2)}{\sqrt{\pi} \Gamma(d/2 + k)} \quad (11)$$

Each solid segment from  $a$  to  $b$  contributes a factor  $e^{-\gamma_R |a-b|}$ , each blank from  $s_k$  to  $t_{k-1}$  contributes  $P(s_k, t_{k-1})$  (note that  $t_k$  always connects to  $s_k$ ), each solid segment passing  $2k$  points contributes a factor  $M_d^k$ ,

and finally there is an extra factor  $p$ . To summarize, we need to sum over  $2^3$  similar diagrams to get the correlation function of order eight.

What remains now is to evaluate the required integrals. All the integrands are products of exponential functions, and are in fact convolutions, noting the identity:

$$2lt - \sum_{k=1}^l (t_k + s_k) = 2l(t - t_l) + \sum_{k=1}^l (2k - 1)(t_k - s_k) + \sum_{k=1}^{l-1} 2k(s_{k+1} - t_k) \quad (12)$$

For the case of, e.g.,  $l = 2$  we remain with two possible diagrams:

$$\bullet - \bullet - \bullet - \bullet, \quad \text{and} \quad \bullet - \bullet \quad \bullet - \bullet \quad (13)$$

and the corresponding moments can be obtained as

$$\begin{aligned} \langle (\tilde{x}^4)(\xi) \rangle &= \frac{4v^4 p}{\xi(4b + \xi)} \frac{3}{\gamma(1-p) + 3b + \xi} \frac{2}{\gamma(1-p) + 2b + \xi} \frac{1}{\gamma(1-p) + b + \xi} \frac{3}{d^2 + 2d} \\ &+ \frac{4v^4 p}{\xi(4b + \xi)} \frac{3}{\gamma(1-p) + 3b + \xi} \left( \frac{2p}{2b + \xi} + \frac{2(1-p)}{\gamma + 2b + \xi} - \frac{2}{\gamma(1-p) + 2b + \xi} \right) \frac{1}{\gamma(1-p) + b + \xi} \frac{1}{d^2} \end{aligned} \quad (14)$$

where  $\xi$  is the Laplace transform variable. In principle, all the moments are rational functions of  $\xi$  and thus the inverse Laplace transform can be obtained. In reality, such expressions would soon become unwieldy as one goes to higher order. However, the limit  $t \rightarrow \infty$ , corresponding to the steady state, can still be easily calculated, using the fact that:

$$\lim_{t \rightarrow \infty} f(t) = \lim_{\xi \rightarrow 0} \xi \tilde{f}(\xi) \quad (15)$$

The limit on the r.h.s. is trivial as seen from the above example.

### C. Volterra difference equation

From the diagram law, we may derive a programmable Volterra difference equation that avoids calculating all the  $2^{l-1}$  diagrams for  $2l$  moment and considerably simplifies the calculation.

It can be noticed that the part to the right (but not to the left) of any blank in a diagram, is itself also a

diagram, and a factor of the whole diagram, so one can break any diagram from the leftmost blank. Thus if one sets

$$L^l(\xi) = \frac{\langle (\tilde{x}^{2l})(\xi) \rangle \xi(2lb + \xi)}{2lv^{2l}p} \quad (16)$$

one can obtain:

$$L^l(\xi) = \sum_{k=1}^{l-1} \left( \prod_{m=2k+1}^{2l-1} \frac{m}{\gamma_R + mb + \xi} \right) g_k L^k(\xi) M_d^{l-k} + \prod_{m=+1}^{2l-1} \frac{m}{\gamma_R + mb + \xi} M_d^l \quad (17)$$

where:

$$g_k = \frac{2kp}{2kb + \xi} + \frac{2k(1-p)}{\gamma + 2kb + \xi} - \frac{2k}{\gamma(1-p) + 2kb + \xi} = \frac{2k\gamma_T\gamma_R}{(\gamma_R + \gamma_T + 2kb + \xi)(\gamma_R + 2kb + \xi)(2kb + \xi)} \quad (18)$$

The name Volterra difference equation comes from

the fact that it may be regarded as the discrete coun-

terpart of the Volterra integral equation. While difficult to solve in general, the Volterra difference equation has the advantage that r.h.s. requires only  $L^k$  up to  $k = l - 1$ , and thus we can calculate the moment  $\langle (x^{2l}) (\xi) \rangle$  recursively. Starting with:

$$L^1 (\xi) = \frac{1}{\gamma_R + b + \xi} M_d^1 \quad (19)$$

we may recursively calculate all  $L^k$  up to  $k = l$ , then recover the moment using Eq. 16.

#### D. General results

While we are considering a RTP in a harmonic trap, it is possible to consider the RTP in free space by setting  $b = 0$ , and obtain the time-dependent distribution in terms of Fourier-Laplace transform as in [22]. Define:

$$K^l (\xi) = \frac{\langle (x^{2l}) (\xi) \rangle \xi^2}{(2l)! v^{2l} p} \quad (20)$$

$$f_l = \prod_{m=+1}^{2l-1} \frac{1}{\gamma_R + \xi} = \frac{1}{(\gamma_R + \xi)^{2l-1}} \quad (21)$$

with

$$h = \frac{\gamma_T \gamma_R}{(\gamma_R + \gamma_T + \xi) \xi} \quad (22)$$

The Volterra difference equation for  $K^l$  can be arranged into:

$$\frac{K^{l+1}}{f_{l+1}} = \sum_{k=0}^l \frac{1}{f_k} h K^k (\xi) M_d^{l+1-k} + M_d^{l+1} - \frac{h K^0 (\xi)}{f_0} M_d^{l+1}. \quad (23)$$

The crucial simplification here is that  $h$  does not depend on  $k$ , unlike the case  $b > 0$ , and thus this equation is of the convolution type. Therefore it can be solved by means of the Z-transform [45]:

$$\hat{A}(z) = Z(A(n)) = \sum_{j=0}^{\infty} A(j) z^{-j} \quad (24)$$

The explicit form of the Z-transform is then obtained as  $M_d^l$ :

$$\hat{M}_d(z) = {}_2F_1 \left( 1, \frac{3}{2}; 1 + \frac{d}{2}; \frac{1}{z} \right) \quad (25)$$

and it is possible to solve Eq. 23 as

$$Z \left( \frac{K^l}{f_l} \right) (z) - \frac{K^0}{f_0} = \frac{{}_2F_1 \left( 1, \frac{3}{2}; 1 + \frac{d}{2}; \frac{1}{z} \right)}{z - h {}_2F_1 \left( 1, \frac{3}{2}; 1 + \frac{d}{2}; \frac{1}{z} \right)} \quad (26)$$

We then calculate the characteristic function by expanding and interchanging the order of summation and expectation. Note that:

$$\sum_{l=1}^{\infty} \left( \frac{i\omega v}{\gamma_R + \xi} \right)^{2l} \frac{K^l}{f_l} = Z \left( \frac{K^l}{f_l} \right) \left( -\frac{(\gamma_R + \xi)^2}{\omega^2 v^2} \right) - \frac{K^0}{f_0} \quad (27)$$

It is therefore not necessary to carry out the inverse Z-transform, and we can obtain directly:

$$\langle e^{i\omega x} \rangle = \frac{1}{\xi} - \frac{1}{\xi^2} \frac{p(\gamma_R + \xi) {}_2F_1 \left( 1, \frac{3}{2}; 1 + \frac{d}{2}; -\left( \frac{\omega v}{\gamma_R + \xi} \right)^2 \right)}{\frac{(\gamma_R + \xi)^2}{\omega^2 v^2} + h {}_2F_1 \left( 1, \frac{3}{2}; 1 + \frac{d}{2}; -\left( \frac{\omega v}{\gamma_R + \xi} \right)^2 \right)} \quad (28)$$

For the special case of  $d = 1, 2, 3$ , which can be furthermore checked to agree with [22].

So far we have been considering the distribution of one coordinate components, *i.e.*, a RTP in a potential  $\sim x^2/2$ , with active velocities in  $d$  dimensions but the potential only in one dimension. For  $d > 1$ , one may wish to consider the distribution of the vector  $r$  instead of one of its coordinate components  $x$ . Assuming spherical symmetry, we only need the distribution of  $|r|$  or  $|r|^2$ . We could convert the moments for  $x$  into moments of  $|r|^2$  as:  $\langle (x)^{2l} \rangle = m_d^l \langle |r|^{2l} \rangle$ , where  $m_d^l = \Gamma(1/2 + l) \Gamma(d/2) / (\sqrt{\pi} \Gamma(d/2 + l))$  is the  $2l$  moment of coordinate components for a random vector uniformly chosen from a  $d - 1$  dimension unit sphere. In our problem  $m$  coincides with  $M$  but in general they may be different. These are already known from [31, 32] and we need not go further here.

One interesting feature of the RTP is that it may cluster near the boundary. Here we show such cluster at a single particle level, which depends only on the rate of the run state  $\gamma_R = (1 - p)\gamma$ . Numerically we find that, for the steady state, as  $l \rightarrow \infty$ :

$$\langle (x)^{2l} \rangle \propto l^{-\gamma_R - \frac{d-1}{2}} \quad (29)$$

Notice that the last term in the Volterra difference equation  $\prod_{m=+1}^{2l-1} \frac{m}{\gamma_R + mb} M_d^l$  has the same scaling law. The first implication is that, since the moments are asymptotically decreasing, the distribution must be supported in  $[-1, 1]$ . Furthermore, by the same argumentation as in Ref. [46], as  $x$  approaches the boundary, the density will approach:

$$p(x) \propto (1 - |x|)^{\gamma_R + \frac{d-1}{2} - 1}. \quad (30)$$

Therefore, we conclude that if  $p(1) = 0$  or  $p(1) \rightarrow \infty$ , then  $\gamma_R > (1-d)/2$  and  $\gamma_R < (1-d)/2$ , respectively. For  $d = 2$  the critical value is  $1/2$  and for  $d = 3$  it is  $0$ . Thus we may conclude that in 3d, the distribution of coordinate component is not singular near the boundary. However, the distribution of  $r^2$  might still be singular.

### E. Active Brownian particles

While not the focus of this paper, it is worthwhile to mention that the methodology described above can be adapted to the (2D) Active Brownian particles (ABP) [33] as well, with active velocities diffusing along a circle. The equation of motion for the ABP is:

$$\dot{x}(t) = -bx(t) + v \cos \theta(t) \quad (31)$$

$$\dot{\theta}(t) = \sqrt{2D}\eta \quad (32)$$

Where  $D$  is the diffusion constant and  $\eta$  is the standard Gaussian white noise. We then again use the solution:

$$x(t) = v \int_0^t \cos \theta(s) e^{-b(t-s)} ds \quad (33)$$

(with  $x(0) = \theta(0) = 0$ ) to calculate the moments:

$$\langle r(t)^l \rangle = v^l l! \int_{0 \leq t_1 \leq \dots \leq t_l \leq t} dt_i e^{-b(t - \sum_k t_k)} \left\langle \prod_k \cos \theta(t_k) \right\rangle = \frac{v^l l!}{2^l} \sum_{a_i = \pm 1} \int_{0 \leq t_1 \leq \dots \leq t_l \leq t} dt_i e^{-b(t - \sum_k t_k)} \langle e^{\sum_k i a_k \theta(t_k)} \rangle \quad (34)$$

Using the standard identity valid for Gaussian variables

$$\langle e^A \rangle = e^{\langle A \rangle + \frac{1}{2}(\langle A^2 \rangle - \langle A \rangle^2)},$$

and the correlation function  $\langle \theta(t_i) \theta(t_j) \rangle = 2D \min(t_i, t_j)$ , it can be checked that:

$$\langle e^{\sum_k i a_k \theta(t_k)} \rangle = e^{-D \sum_{k=0}^{l-1} (t_{k+1} - t_k) (\sum_{i=k+1}^l a_i)^2}, \quad (35)$$

where we use the convention  $t_0 = 0$ . Together with the identity Eq. 12, we see that Eq. 34 is again a convolution, and the corresponding Laplace transform is:

$$\langle \tilde{x}(\xi)^l \rangle = \frac{v^l l!}{2^l} \sum_{a_i = \pm 1} \prod_{k=0}^{l-1} \frac{1}{D \left( \sum_{i=k+1}^l a_i \right)^2 + bk + \xi}, \quad (36)$$

where it is understood that  $\sum_{i=l+1}^l \dots = 0$ . The steady state moments agree with the examples given in [33].

### III. 1D: EXACT STEADY STATE DISTRIBUTION

One specific case where the problem can be drastically simplified is when  $M_d^l = (M_d^1)^l$ . The problem of 1D

run and tumble is one such case where  $M_1^l = 1$ . In this case, all non-zero diagrams of the same order contribute the same, and Eq. 17 then results in an explicit expression for any order of moments. Therefore, by expanding  $e^{i\omega x}$  and exchanging the order of summation and expectation, we obtain the characteristic function for steady state distribution in the form:

$$\langle e^{i\omega x} \rangle = {}_1F_2 \left( \frac{\gamma_T}{2b}; \frac{\gamma_R + \gamma_T}{2b}, \frac{1}{2} + \frac{\gamma_R}{2b}; -\frac{v^4 \omega^2}{4b^2} \right) \quad (37)$$

Where  ${}_1F_2$  is the hypergeometric function. Noticing that  $\langle e^{i\omega x} \rangle$  is the Fourier transform of the distribution function  $p(x)$ , we can carry out the inverse Fourier transform. For simplicity we rescale the time so that  $b = 1$ , then rescale space so that  $v = 1$ . Under these conditions, the steady state distribution function becomes, for  $|x| < 1$  (otherwise zero):

$$p(x) = \frac{\sqrt{\pi} \Gamma \left( \frac{\gamma_R + \gamma_T}{2} \right) \Gamma \left( \frac{1 + \gamma_R}{2} \right)}{\Gamma \left( \frac{\gamma_T}{2} \right) \Gamma \left( \frac{\gamma_R}{2} \right) \cos \frac{\pi \gamma_T}{2}} \left\{ \frac{|x|^{\gamma_T - 1} {}_2F_1 \left( \frac{2 - \gamma_R}{2}, \frac{1 - \gamma_R + \gamma_T}{2}; \frac{1 + \gamma_T}{2}; x^2 \right)}{\Gamma \left( \frac{1 + \gamma_R - \gamma_T}{2} \right) \Gamma \left( \frac{1 + \gamma_T}{2} \right)} - \frac{{}_2F_1 \left( \frac{2 - \gamma_R}{2}, \frac{3 - \gamma_R - \gamma_T}{2}; \frac{3 - \gamma_T}{2}; x^2 \right)}{\Gamma \left( \frac{\gamma_R + \gamma_T - 1}{2} \right) \Gamma \left( \frac{3 - \gamma_T}{2} \right)} \right\} \quad (38)$$

First, in general, the hypergeometric function  ${}_2F_1(\cdot, \cdot; \cdot; x)$  converges only for  $|x| < 1$ . This is precisely the region in which the particle will be bounded, as discussed in Subsection II A.

We then check our result by taking the limit  $\gamma_T \rightarrow \infty$ . We work with the characteristic function since the distribution is more complicated. We notice that with large  $\gamma_T$ , the first two parameters of the characteristic function becomes the same, therefore the hypergeometric function will be reduced into

$$\langle e^{i\omega x} \rangle = {}_0F_1\left(\frac{1 + \gamma_R}{2}; -\frac{\omega^2}{4}\right) \quad (39)$$

We then perform the inverse Fourier transform:

$$p(x, \gamma_T \rightarrow \infty) = \frac{2\Gamma\left(\frac{3+\gamma_R}{2}\right) (1-x^2)^{\gamma_R/2-1}}{\sqrt{\pi} (1+\gamma_R) \Gamma\left(\frac{\gamma_R}{2}\right)} \quad (40)$$

This agrees with the well known result in, e.g., [34, 35], except that  $2\gamma_R$  is the actual run rate as defined in

---


$$p(x) \propto \left( {}_2F_1\left(\frac{2-\gamma_R}{2}, \frac{2-\gamma_R}{2}; 1; x\right) \left( \ln|x| + \gamma_E + \frac{\Gamma'\left(\frac{\gamma_R}{2}\right)}{\Gamma\left(\frac{\gamma_R}{2}\right)} \right) + \left( {}_2F_1^{(0,1,0,0)} + {}_2F_1^{(0,0,1,0)} \right) \left( \frac{2-\gamma_R}{2}, \frac{2-\gamma_R}{2}, 1, x \right) \right), \quad (42)$$


---

leading to a logarithmic singularity near the center.

In addition, we find numerically that for  $\gamma_T > 2$ ,  $p'(0) = 0$ , whereas when  $\gamma_T < 2$ , the derivative does not exist. In general, it seems the  $k-1$  derivative at 0 exists iff  $\gamma_T > k$ , while the odd order derivative is zero due to symmetry.

Similarly,  $\gamma_R < 1$  results in singular peaks near the boundaries, whereas for  $\gamma_R > 1$ ,  $p(1) = 0$ . This can be proved by the scaling law of moments Eq. 29. If  $\gamma_R = 1$  the behavior will depend on  $\gamma_T$ : for  $\gamma_T < 2$ ,  $p(1)$  is finite, whereas for  $\gamma_T > 2$ , it diverges. For  $\gamma_R = 1, \gamma_T = 2$ , one has a uniform distribution  $p(x) = 1/2$ . In addition, the derivatives at boundaries exhibit a similar behavior to the derivatives at center: the  $k-1$  derivative at 1 exists iff  $\gamma_R > k$ . Furthermore, when the derivative exists, it is always zero.

Unfortunately, such trick is almost exclusive to 1d, since from the requirement  $M_d^l = (M_d^1)^l$ , one can calculate its characteristic function, and after the inverse Laplace transform, one can show such distribution is the Bernoulli distribution. Therefore, the method here is applicable to 1D or to a simple direct product of 1d (like in [30]).

some references. The extra factor of 2 does not appear in  $d > 1$ .

Next we compare our results with [43], where it has been found that if  $\gamma_R = \gamma_T > 1$ , the distribution is continuous; whereas when  $\gamma_R = \gamma_T < 1$ , the distribution would exhibit three poles, located at the center and the two boundaries. Our results here allow for the case  $\gamma_R \neq \gamma_T$ , and it has been found that the singularities near the center and the boundaries are controlled independently by  $\gamma_T$  and  $\gamma_R$ , respectively.

More specifically,  $\gamma_T \leq 1$  results in a singular peak near the center, whereas for  $\gamma_T > 1, \gamma_R < \infty$ ,  $p(0)$  is always finite, although it might be very large for large  $\gamma_R$ . This can be shown from the expansion of  $p$  near 0, assuming  $\gamma_T < 2$ :

$$p(x) \propto \frac{|x|^{\gamma_T-1}}{\Gamma\left(\frac{1+\gamma_R-\gamma_T}{2}\right) \Gamma\left(\frac{1+\gamma_T}{2}\right)} - \frac{1}{\Gamma\left(\frac{\gamma_R+\gamma_T-1}{2}\right) \Gamma\left(\frac{3-\gamma_T}{2}\right)} + O(x) \quad (41)$$

Thus the case  $\gamma_T \neq 1$  is obvious. Case  $\gamma_T = 1$  may be considered as the limit  $\gamma_T \rightarrow 1$ :

#### IV. STEADY STATE DISTRIBUTION: GAUSSIAN QUADRATURE

Without the simplification in Section III, the exact solutions are difficult to find. Yet we may still approximate the distribution from its finitely-many moments that can be calculated at least numerically. Extracting information about distribution from its moments is a century-old problem in mathematics referred to as the moment problem [47]. While theories about the existence of the distribution and some estimations in terms of inequalities can be found, it seems that an adequate approach in practice is still lacking. In [33] the practical problem was solved by expanding the distribution in terms of the Legendre polynomials. However, such approach only works well when the distribution is smooth, whereas in our case, the distribution may be singular, resulting in a slow convergence. Thus we approach this problem via another route, by considering the Gaussian quadrature corresponding to the distribution, i.e., we start with an approximation of the expectation of any smooth function  $f$ , using the value of  $f$  on specific points:

$$\langle f \rangle \approx \sum_{j=0}^N u_j f(x_j) \quad (43)$$

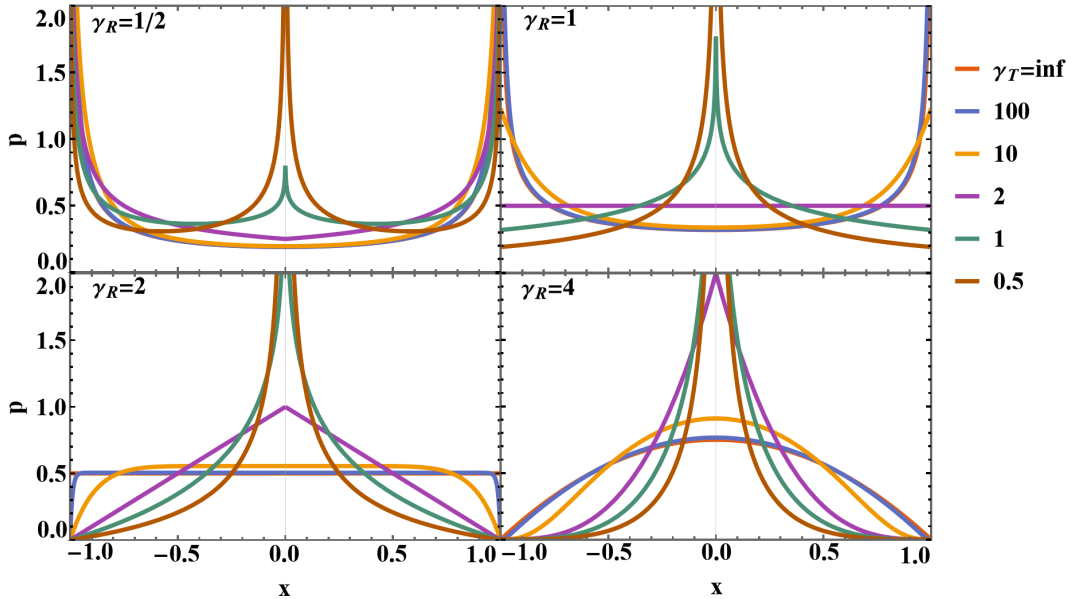


Figure 2. Examples of exact steady state distribution for a RTP in a harmonic trap with finite tumble time in 1D, according to Eq. 38. The harmonic potential strength  $b$  and the active velocity  $v$  are both rescaled to 1. The run rates are  $\gamma_R = 1/2, 1, 2, 4$  respectively. In each graph the legend gives the value of the tumble rate  $\gamma_T$ .

We rescale the time and length such that  $b = v = 1$ . Then  $x$  will lie between  $-1$  and  $1$ . One practical way to evaluate the expectation of  $f$  supported within  $[-1, 1]$ , is to expand  $f$  in the Chebyshev polynomials, and evaluate the expectation of the Chebyshev polynomials using the moments. The Chebyshev polynomials are an excellent choice for expanding the continuous functions on closed intervals using polynomials, due to its exponential convergence rate, explicit grids, minimal amplitude and thus low uniform error (compared with other orthonormal polynomials) [48].

The Chebyshev approximation can be explicitly constructed by the values of  $f$  on the Gauss-Lobatto grids: define  $x_i = \cos \frac{\pi i}{N}$ ;  $p_i = 2$  if  $i = 0$  or  $i = N$ , otherwise  $p_i = 1$ ;  $J_{ij} = \frac{2}{p_i p_j N} \cos \frac{\pi i j}{N}$ , then the Chebyshev approximation is

$$f(x) \approx \sum_{i,j=0}^N J_{ij} f(x_j) T_i(x) \quad (44)$$

where  $T_n(\cos \theta) = \cos n\theta$  is the  $n$ -th Chebyshev polynomial (of the first kind). Taking the average on both sides, we have:

$$\langle f \rangle \approx \sum_{i,j=0}^N J_{ij} \langle T_i(x) \rangle f(x_j) \quad (45)$$

This indeed gives us the Gaussian quadrature with the abscissas being  $x_j$  and the weights being  $w_j = \sum_{i=0}^N J_{ij} \langle T_i(x) \rangle$ . In our problem, the expectation of Chebyshev polynomials can be evaluated exactly from

the moments, and thus the error comes only from the Chebyshev approximation, which decays exponentially and uniformly over the whole region.

On the other hand, suppose we could continuously extend  $x_j$  such that  $j$  is allowed to be real number, then we have:

$$\langle f \rangle = \int f(x(j)) p(x(j)) \frac{dx}{dj} dj, \quad (46)$$

assuming that  $p$  is smooth near  $x_j$ . We choose  $f$  to be non-zero only near  $x_j$ , such that:

$$\langle f \rangle \approx p(x_j) \frac{dx_j}{dj} \approx \sum_{i=0}^N J_{ij} \langle T_i(x) \rangle \quad (47)$$

Since we know  $|\partial_i x_i| = \frac{\pi}{N} |\sin \frac{\pi i}{N}|$ , we obtain an approximate distribution at discrete points:

$$p\left(\cos \frac{\pi j}{N}\right) \sim \sum_{i=0}^N \frac{J_{ij} \langle T_i(x) \rangle}{\frac{\pi}{N} |\sin \frac{\pi j}{N}|} \quad (48)$$

The behavior near the boundary agrees with our conclusion in Subsection II D. The behavior near the center is more complicated. Our argument is only correct if distribution  $p$  is smooth near  $x_j$ , thus the points given at the center may not be correct.

## V. CONCLUSION

Typically the study of many stochastic processes has focused on the Fokker-Planck equation. The Langevin



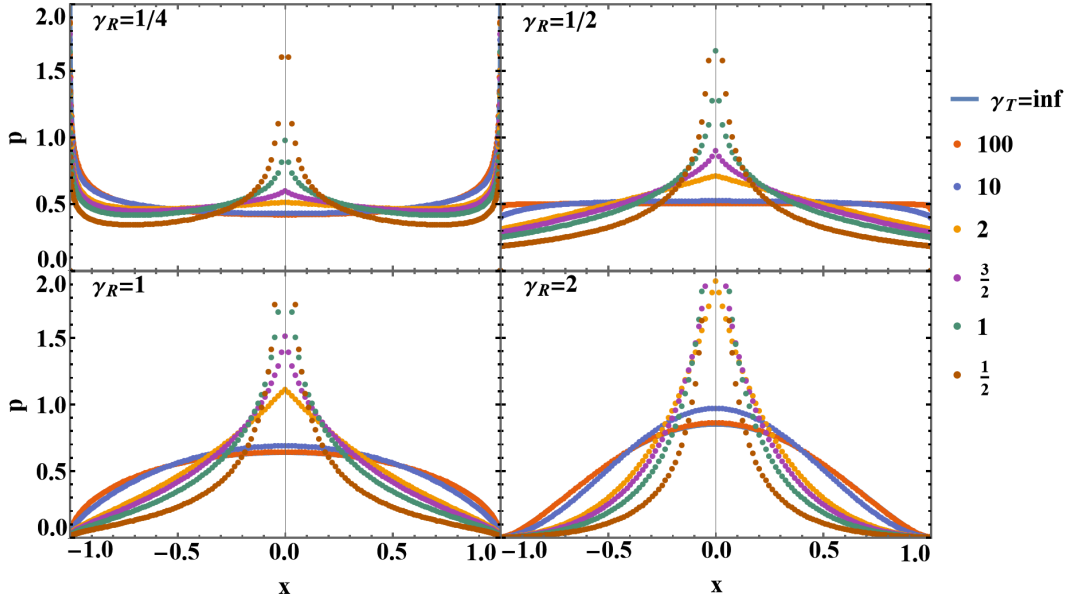


Figure 3. Approximated distribution from the Gaussian quadrature for a RTP in the harmonic trap with finite tumble time in  $2D$ . The harmonic potential  $b$  and the active velocity  $v$  are rescaled to 1. The run rates are  $\gamma_R = 1/4, 1/2, 1, 2$  respectively. In each graph the legends gives the value of  $\gamma_T$ . The solid lines represent the exact distribution for  $\gamma_T \rightarrow \infty$

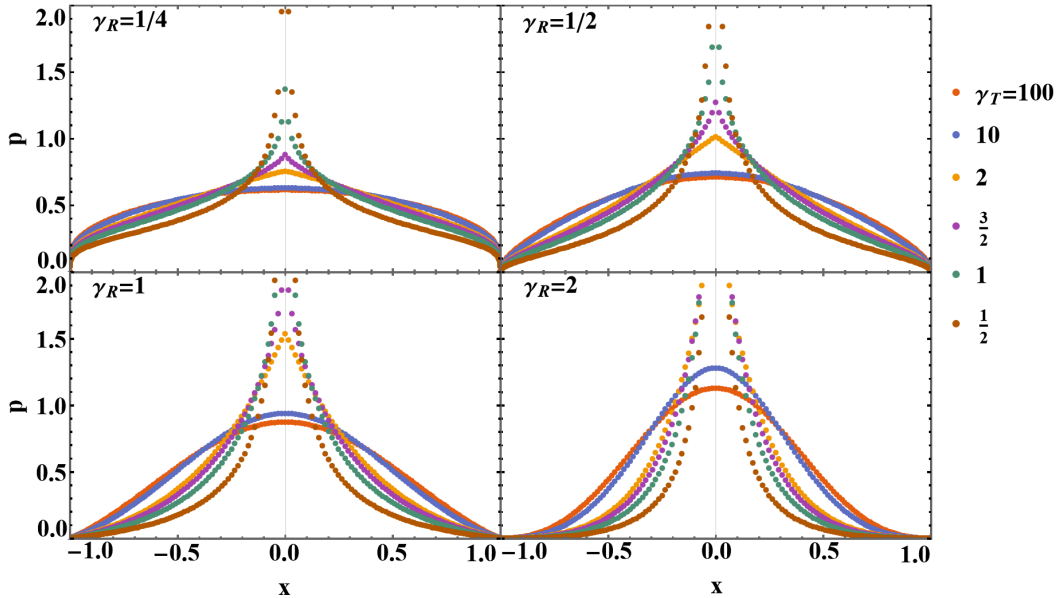


Figure 4. Approximated distribution from Gaussian quadrature for a RTP in the harmonic trap with finite tumble time in  $3D$ . The harmonic potential  $b$  and the active velocity  $v$  are rescaled to 1. The run rates are  $\gamma_R = 1/4, 1/2, 1, 2$  respectively. In each graph the legends gives the value of  $\gamma_T$ .

equation, or the equation of motion, has been more or less overlooked, so that sometimes it is not even explicitly written down. Yet in this work, it seems fair to claim that at least for some problems, the equation of motion itself can be quite powerful, leading to results that are not easily derived from the corresponding Fokker-Planck equation.

Guided by the seminal work of Mark Kac [44], we calculated the moments of RTP in a harmonic poten-

tial with finite tumble time, using the diagram laws and the programmable Volterra difference equation, derived from the equation of motion. In 1D, we obtain the exact steady state distributions, generalizing the previous results [43] to arbitrary choice of  $\gamma_R$  and  $\gamma_T$ . In 2D and 3D, we approximate the distribution from the moments via the Gaussian quadrature, extending the results from [31, 32] to the cases with a finite tumble time.

Nevertheless, questions still remain. The first unre-

solved question is, what more can we learn from the Volterra difference equation. Notice the equation is almost a convolution, and can be solved exactly for  $b = 0$ , therefore it might be amenable to further manipulation for  $b \neq 0$ .

The second question is whether the steady state of a 2D RTP in a harmonic trap can be solved in general. As noted by [31, 32], although possibly difficult to derive, the moments for the steady state distribution of 2D RTP with zero tumble time can be inferred easily:

$$L_i^l(0) = M_d^l \prod_{m=1}^l \frac{m}{\gamma_R + m}, \quad (49)$$

and thus the exact steady state distribution can be calculated. Also note that the characteristic function for the 1D and 2D cases with zero tumble time are very similar: in 1D,

$$\langle e^{i\omega x} \rangle = {}_0F_1 \left( \frac{1 + \gamma_R}{2}; -\frac{\omega^2}{4} \right) \quad (50)$$

whereas in 2D:

$$\langle e^{i\omega x} \rangle = {}_0F_1 \left( 1 + \gamma_R; -\frac{\omega^2}{4} \right) \quad (51)$$

Is it possible to derive the distribution with a finite tumble time? Note that, in 2D, one may use a complex formalism to trade the difficulty in  $M$ , to a combinatorial problem. Can one obtain more insights by this approach?

The third question is the time dependent problem. In principle we are solving the problem for any time, yet at the end, due to the difficulty in the inverse Laplace transform, only the infinite time, *viz.*, steady state distribution is obtained. It would be interesting to consider other times as well. The moments are all rational in the Laplace parameter  $\xi$ , thus in principle there is no difficulty to obtain the inverse. In practice, however, the results will be complicated.

Another question is whether such approach can be generalized to some other problems. One such possibility is that the velocity would be biased in one direction. Also possible is a more complex Markov chain for  $R$  to model other problems in the general theory of stochastic phenomena. A good example remains to be found. Furthermore, it would be interesting to consider a harmonic potential, or to include the interaction of particles, though it is unclear how to achieve this since we need the explicit solution to the equation of motion.

Finally, it would be interesting to apply the Gaussian quadrature method to practical data processing, *e.g.*, inferring the distribution from given data. As long as we can find a scheme to approximate any smooth function  $f$  supported on the same interval as the distribution function, by grids  $x_j$  and corresponding cardinal functions

$C_j$  (where  $C_j = \sum_{i=0}^N J_{ij} T_i(x)$  in our Chebyshev expansion), our argument seems to hold. Thus by calculating the expectation of the cardinal functions from the data, it seems possible to estimate  $p(x_j)$ . Furthermore, assuming  $p$  itself is smooth, then it can be expanded using the same cardinal functions  $C_j$ , and the coefficients we need in such expansion are exactly  $p(x_j)$  that we just estimated.

## VI. ACKNOWLEDGMENTS

The authors would like to thank D. Frydel for his insightful comments on an earlier version of the manuscript. FY acknowledges the support of the National Natural Science Foundation of China (Grant No. 12090054 and 12325405) and the Strategic Priority Research Program of Chinese Academy of Sciences (Grant No. XDB33030300). RP acknowledges the support of the Key project of the National Natural Science Foundation of China (NSFC) (Grant No. 12034019).

---

\* Corresponding author. podgornikrudolf@ucas.ac.cn.

- [1] M. C. Marchetti, J. F. Joanny, S. Ramaswamy, T. B. Liverpool, J. Prost, Madan Rao, and R. Aditi Simha. Hydrodynamics of soft active matter. *Reviews of Modern Physics*, 85(3):1143–1189, July 2013.
- [2] Clemens Bechinger, Roberto Di Leonardo, Hartmut Löwen, Charles Reichhardt, Giorgio Volpe, and Giovanni Volpe. Active particles in complex and crowded environments. *Reviews of Modern Physics*, 88(4):045006, November 2016.
- [3] Étienne Fodor, Robert L. Jack, and Michael E. Cates. Irreversibility and biased ensembles in active matter: Insights from stochastic thermodynamics. *Annual Review of Condensed Matter Physics*, 13(1):215–238, March 2022.
- [4] F Backouche, L Haviv, D Groswasser, and A Bernheim-Groswasser. Active gels: dynamics of patterning and self-organization. *Physical Biology*, 3(4):264–273, December 2006.
- [5] Daisuke Mizuno, Catherine Tardin, C. F. Schmidt, and F. C. MacKintosh. Nonequilibrium mechanics of active cytoskeletal networks. *Science*, 315(5810):370–373, January 2007.
- [6] Howard C. Berg. *E. coli in Motion*. Biological and Medical Physics, Biomedical Engineering. Springer New York, New York, NY, 1st ed. 2004. edition, 2004.
- [7] Claire Wilhelm. Out-of-equilibrium microrheology inside living cells. *Physical Review Letters*, 101(2):028101, July 2008.
- [8] Lee Walsh, Caleb G. Wagner, Sarah Schlossberg, Christopher Olson, Aparna Baskaran, and Narayanan Menon. Noise and diffusion of a vibrated self-propelled granular particle. *Soft Matter*, 13(47):8964–8968, 2017.
- [9] Sriram Ramaswamy. The mechanics and statistics of active matter. *Annual Review of Condensed Matter Physics*, 1(1):323–345, August 2010.

- [10] Nitzan Razin, Raphael Voituriez, and Nir S. Gov. Signatures of motor susceptibility to forces in the dynamics of a tracer particle in an active gel. *Physical Review E*, 99(2):022419, February 2019.
- [11] Simon Hubbard, Petro Babak, Sven Th. Sigurdsson, and Kjartan G. Magnússon. A model of the formation of fish schools and migrations of fish. *Ecological Modelling*, 174(4):359–374, June 2004.
- [12] John Toner, Yuhai Tu, and Sriram Ramaswamy. Hydrodynamics and phases of flocks. *Annals of Physics*, 318(1):170–244, July 2005.
- [13] Nitin Kumar, Harsh Soni, Sriram Ramaswamy, and A. K. Sood. Flocking at a distance in active granular matter. *Nature Communications*, 5(1), September 2014.
- [14] G. Du, S. Kumari, F. Ye, and R. Podgornik. Model of metameric locomotion in smooth active directional filaments with curvature fluctuations. *Europhysics Letters*, 136(5):58003, mar 2022.
- [15] Borge ten Hagen, Felix Kümmer, Raphael Wittkowski, Daisuke Takagi, Hartmut Löwen, and Clemens Bechinger. Gravitaxis of asymmetric self-propelled colloidal particles. *Nature Communications*, 5(1), September 2014.
- [16] Sho C. Takatori, Raf De Dier, Jan Vermant, and John F. Brady. Acoustic trapping of active matter. *Nature Communications*, 7(1), March 2016.
- [17] A. P. Solon, M. E. Cates, and J. Tailleur. Active brownian particles and run-and-tumble particles: A comparative study. *The European Physical Journal Special Topics*, 224(7):1231–1262, July 2015.
- [18] Kai M. Thormann, Carsten Beta, and Marco J. Kühn. Wrapped up: The motility of polarly flagellated bacteria. *Annual Review of Microbiology*, 76(1):349–367, September 2022.
- [19] Tine Curk, Davide Marenduzzo, and Jure Dobnikar. Chemotactic sensing towards ambient and secreted attractant drives collective behaviour of e. coli. *PLOS ONE*, 8, 10 2013.
- [20] Ion Santra, Urna Basu, and Sanjib Sabhapandit. Run-and-tumble particles in two dimensions: Marginal position distributions. *Physical Review E*, 101(6):062120, June 2020.
- [21] Francesco Mori, Pierre Le Doussal, Satya N. Majumdar, and Grégory Schehr. Universal survival probability for a d-dimensional run-and-tumble particle. *Physical Review Letters*, 124(9):090603, March 2020.
- [22] L. Angelani. Averaged run-and-tumble walks. *EPL (Europhysics Letters)*, 102(2):20004, April 2013.
- [23] Michael E. Cates and Julien Tailleur. Motility-induced phase separation. *Annual Review of Condensed Matter Physics*, 6(1):219–244, March 2015.
- [24] A. B. Slowman, M. R. Evans, and R. A. Blythe. Jamming and attraction of interacting run-and-tumble random walkers. *Physical Review Letters*, 116(21):218101, May 2016.
- [25] Pierre Le Doussal, Satya N. Majumdar, and Grégory Schehr. Noncrossing run-and-tumble particles on a line. *Physical Review E*, 100(1):012113, July 2019.
- [26] Prashant Singh and Anupam Kundu. Generalised ‘arcsine’ laws for run-and-tumble particle in one dimension. *Journal of Statistical Mechanics: Theory and Experiment*, 2019(8):083205, August 2019.
- [27] Jens Elgeti and Gerhard Gompper. Run-and-tumble dynamics of self-propelled particles in confinement. *EPL (Europhysics Letters)*, 109(5):58003, March 2015.
- [28] Pierre Le Doussal, Satya N. Majumdar, and Grégory Schehr. Velocity and diffusion constant of an active particle in a one-dimensional force field. *Europhysics Letters*, 130(4):40002, May 2020.
- [29] Oded Farago and Naftali R. Smith. Confined run-and-tumble particles with non-markovian tumbling statistics. *Physical Review E*, 109(4):044121, April 2024.
- [30] Naftali R. Smith, Pierre Le Doussal, Satya N. Majumdar, and Grégory Schehr. Exact position distribution of a harmonically confined run-and-tumble particle in two dimensions. *Physical Review E*, 106(5):054133, November 2022.
- [31] Derek Frydel. Positing the problem of stationary distributions of active particles as third-order differential equation. *Physical Review E*, 106(2):024121, August 2022.
- [32] Derek Frydel. Run-and-tumble oscillator: Moment analysis of stationary distributions. *Physics of Fluids*, 35(10), October 2023.
- [33] Derek Frydel. Active oscillator: Recurrence relation approach. *Physics of Fluids*, 36(1), January 2024.
- [34] A. P. Solon, Y. Fily, A. Baskaran, M. E. Cates, Y. Kafri, M. Kardar, and J. Tailleur. Pressure is not a state function for generic active fluids. *Nature Physics*, 11(8):673–678, June 2015.
- [35] Abhishek Dhar, Anupam Kundu, Satya N. Majumdar, Sanjib Sabhapandit, and Grégory Schehr. Run-and-tumble particle in one-dimensional confining potentials: Steady-state, relaxation, and first-passage properties. *Physical Review E*, 99(3):032132, March 2019.
- [36] Giacomo Gradenigo and Satya N Majumdar. A first-order dynamical transition in the displacement distribution of a driven run-and-tumble particle. *Journal of Statistical Mechanics: Theory and Experiment*, 2019(5):053206, May 2019.
- [37] Prashant Singh, Sanjib Sabhapandit, and Anupam Kundu. Run-and-tumble particle in inhomogeneous media in one dimension. *Journal of Statistical Mechanics: Theory and Experiment*, 2020(8):083207, August 2020.
- [38] Martin R Evans and Satya N Majumdar. Run and tumble particle under resetting: a renewal approach. *Journal of Physics A: Mathematical and Theoretical*, 51(47):475003, October 2018.
- [39] Jaume Masoliver. Telegraphic processes with stochastic resetting. *Physical Review E*, 99(1):012121, January 2019.
- [40] Satya N. Majumdar and Baruch Meerson. Toward the full short-time statistics of an active brownian particle on the plane. *Physical Review E*, 102(2):022113, August 2020.
- [41] Ion Santra, Urna Basu, and Sanjib Sabhapandit. Direction reversing active brownian particle in a harmonic potential. *Soft Matter*, 17(44):10108–10119, 2021.
- [42] Naftali R. Smith. Nonequilibrium steady state of trapped active particles. *Physical Review E*, 108(2):l022602, August 2023.
- [43] Urna Basu, Satya N Majumdar, Alberto Rosso, Sanjib Sabhapandit, and Grégory Schehr. Exact stationary state of a run-and-tumble particle with three internal states in a harmonic trap. *Journal of Physics A: Mathematical and Theoretical*, 53(9):09LT01, February 2020.
- [44] Mark Kac. A stochastic model related to the telegrapher’s equation. *Rocky Mountain Journal of Mathematics*, 4(3), September 1974.
- [45] Saber N. Elaydi, editor. *An Introduction to Difference Equations*. SpringerLink. Springer Science+Business Me-

- dia, Inc, New York, NY, third edition edition, 2005. Includes bibliographical references (p. 523-529) and index.
- [46] L. Touzo, P. Le Doussal, and G. Schehr. Interacting, running and tumbling: The active dyson brownian motion. *Europhysics Letters*, 142(6):61004, June 2023.
- [47] N. I. Akhiezer. *The Classical Moment Problem and Some Related Questions in Analysis*. Society for Industrial and Applied Mathematics, January 2020.
- [48] John P. Boyd. *Chebyshev and Fourier Spectral Methods Second Revised Edition*. Dover Publications, Incorporated, 2013.